International Journal of Geosciences, 2024, 15, 25-39
https://www.scirp.org/journal/ijg
ISSN Online: 2156-8367
ISSN Print: 2156-8359

Estimation of Displacement and Extension due to Reverse Drag of Normal Faults: Forward Method

Shunshan Xu[1], Angel Francisco Nieto-Samaniego[1], Huilong Xu[2*], Susana Alicia Alaniz-Álvarez[1]

[1]Universidad Nacional Autónoma de México, Centro de Geociencias, Apartado Postal 1-742, Querétaro, Qro., México
[2]South China Sea Institute of Oceanology, Chinese Academy of Sciences, Guangzhou, China
Email: *xu630502@163.com

How to cite this paper: Xu, S.S., Nieto-Samaniego, A.F., Xu, H.L. and Alaniz-Álvarez, S.A. (2024) Estimation of Displacement and Extension due to Reverse Drag of Normal Faults: Forward Method. *International Journal of Geosciences*, **15**, 25-39.
https://doi.org/10.4236/ijg.2024.151003

Received: October 30, 2023
Accepted: January 28, 2024
Published: January 31, 2024

Abstract

In the case of reverse drag of normal faulting, the displacement and horizontal extension are determined based on the established equations for the three mechanisms: rigid body, vertical shear and inclined shear. There are three sub-cases of basal detachment for the rigid body model: horizontal detachment, antithetic detachment and synthetic detachment. For the rigid body model, the established equations indicate that the total displacement on the synthetic base (D_{t2}) is the largest, that on the horizontal base (D_{t1}) is moderate, and that on the antithetic base (D_{t3}) is the smallest. On the other hand, the value of (D_{t1}) is larger than the displacement for the vertical shear (D_{t4}). The value of (D_{t1}) is larger than or less than the displacement for the inclined shear (D_{t5}) depending on the original fault dip δ_0, bedding angle θ, and the angle of shear direction β. For all original parameters, the value of D_{t5} is less than the value of D_{t4}. Also, by comparing three rotation mechanisms, we find that the inclined shear produces largest extension, the rigid body model with horizontal detachment produces the smallest extension, and the vertical shear model produces moderate extension.

Keywords

Fault Rotation, Fault Drag, Fault Displacement, Extension, Forward Model

1. Introduction

Anderson's model (1951) [1] predicts dips of normal faults larger than 45˚ [2] and could rotate down to 30˚ during continuous activity [3]. In other words, the normal faults develop progressively, diminishing their dip as the extension proceeds. Because of fault rotation, the beds in faulted blocks also rotate. Drag develops where a layer is oriented at an angle to the slip vector of the fault. Two

ways of bed rotation exist. One is the normal rotation, or normal drag, with beds on the hanging wall dipping in the same direction as that fault in the proximity of faults [4] (**Figure 1(b)**). Normal drag folds may form as a result of frictional drag [5], differential compaction [6], or due to fault-propagation [5] [7] [8]. Small normal drag folds may also form as a result of frictional drag along the fault surface [5]. For the normal drag, antiform is commonly found in the footwalls, whereas synform is observed in the hanging walls of normal faults. Another is the reverse rotation, or reverse drag, with beds on the hanging wall dipping in the opposite direction to the fault [9].

Hamblin (1965) [4] listed several possible mechanisms of reverse drag including multiple stages of deformation, elastic rebound, sagging, inversion of slip directions and differential compaction. The convexity of fault drags may be used to ascertain the sense of slip along faults [10]. Reches and Eidelman (1995) [11] showed by means of numerical modeling that the drag varies from reverse drag at the fault center to normal drag at the termination of the fault. However, Graseman *et al.* (2005) [12] indicated that both normal and reverse drag can develop at the fault center depending on the angle between the markers and the fault; normal drag develops there for low angles (<30˚ - 40˚) and reverse drag for higher angles (**Figure 1**). Drag folds have a smaller wavelength than reverse-drag or rollover folds and may be superimposed on these larger structures [5].

Fault drag is common where there are ductile rocks in the faulted stratigraphy [13] [14] [15]. Drag folds are particularly important in hydrocarbon reservoirs where fault drag changes the communication path across a fault [16] [17] [18] [19]. Also, drag folds can provide useful information to assess earthquake hazards [20]. In this paper, we calculate fault displacement and related extension based on the reverse rotation of normal faults. Its purpose is to compare displacement and extension concerning the three mechanisms of reverse-drag flexures in an effort to determine the origin and significance of this type of structural deformation.

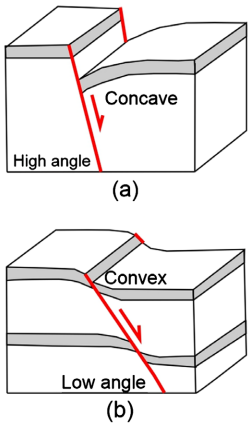

Figure 1. (a) and (b) Fault drag of a central marker along normal faults. The Fault angle is the acute angle measured from the fault to the undeformed central marker (anticlockwise angles are positive).

2. Fault Total Displacement in the Case of Reverse Drag

2.1. Rigid Body Rotation

Reverse-drags are a result of the decrease in displacement with distance from the fault plane. There are three main explanations for bed tilting. One is based on the rigid body rotation model, which assumes that faults bound rigid blocks, the tilt angles of beds and faults are equal and there is no internal deformation within fault blocks (**Figure 2(a)** and **Figure 2(b)**). For this model, the angle of fault rotation (γ_{t1}) is equal to bed tilt (θ),

$$\gamma_{t1} = \delta_0 - \delta_1 = \theta \tag{1}$$

where δ_0 is the original fault dip; δ_1 is the present dip of the fault.

For the rigid body rotation, any line between two faults is not altered, *i.e.* AB′ = L_0, where L_0 is the original horizontal distance between the two faults. The total displacement AD′ can be calculated from triangle AB′D′ by the law of sines.

$$D_{t1} = \mathrm{AD}' = L_0 \frac{\sin\theta}{\sin\delta_1} = \frac{L_0 \sin\theta}{\sin(\delta_0 - \theta)} \tag{2}$$

The above calculation is based on the fact that the basal detachment is horizontal. A more realistic case is that the basal detachment is inclined [21]. If the dip direction of the basal detachment is the same as that of faults, the detachment is synthetic (**Figure 2(c)** and **Figure 2(d)**). If the dip direction of the basal detachment is opposite to that of faults, the detachment is antithetical (**Figure 2(e)** and **Figure 2(f)**). Before rotation in the case of synthetic detachment, by using the law of sines for triangle ABC in **Figure 2(c)**, we obtain

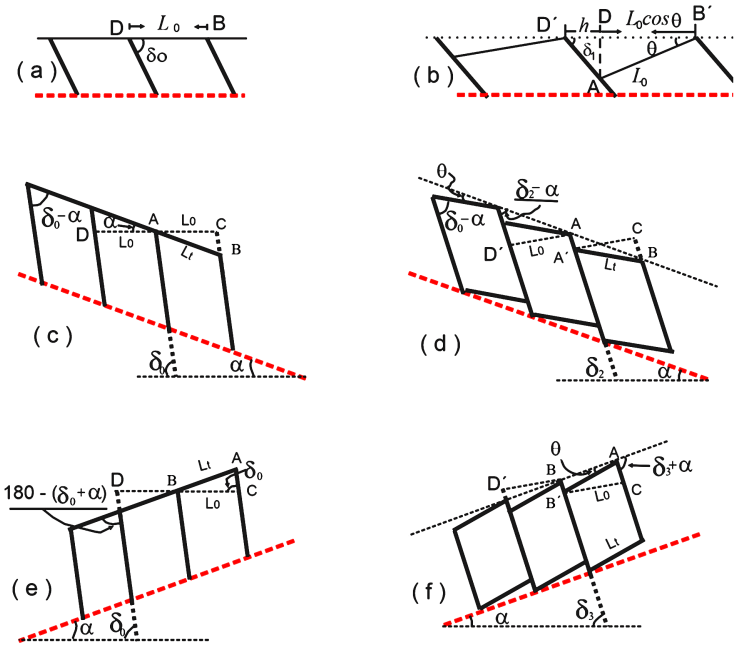

Figure 2. Sketch showing the rigid body model. (a) and (b) The basal detachment is horizontal. (c) and (d) The basal detachment is synthetic. (e) and (f) The basal detachment is antithetical.

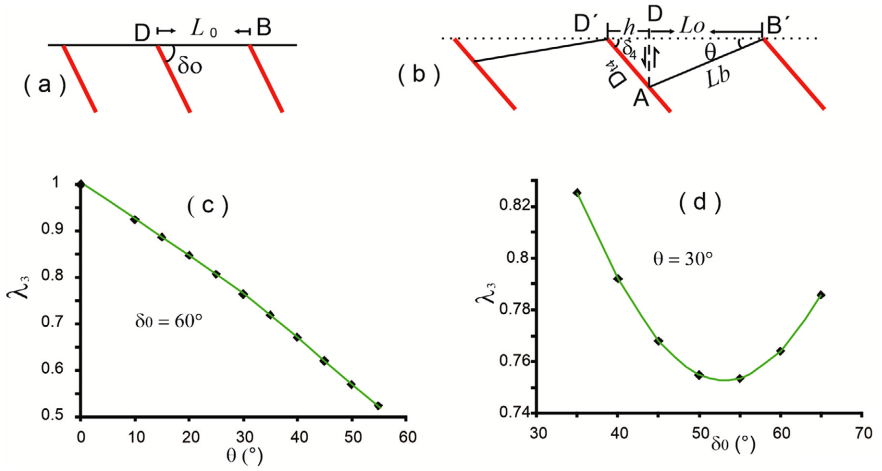

Figure 3. Sketch of vertical shear model. (a) The bedding is horizontal before rotation of normal fault. (b) The bedding is tilted after faulting. The fault dip becomes shallower. The horizontal distance between the footwall cutoff of one fault and the hanging-wall cutoff in the next fault does not change. (c) Given $\delta_0 = 60^\circ$, the value of $\lambda_3 = D_{t4}/D_{t1}$ varies with the angle of θ. (d) Change of $\lambda_3 = D_{t4}/D_{t1}$ with angle of δ_0 for $\theta = 30^\circ$.

$$L_t = \mathrm{AB} = L_0 \frac{\sin(180-\delta_0)}{\sin(\delta_0-\alpha)} = \frac{L_0 \sin\delta_0}{\sin(\delta_0-\alpha)} \tag{3}$$

Likewise, by applying the law of sines to triangle AA B after rotation in Figure 2(d), the total displacement (AA) is determined by

$$D_{t2} = \mathrm{AA}' = L_t \frac{\sin\theta}{\sin(\delta_2-\alpha)} = \frac{L_t \sin\theta}{\sin(\delta_0-\theta-\alpha)} = \frac{L_0 \sin\delta_0 \sin\theta}{\sin(\delta_0-\alpha)\sin(\delta_0-\alpha-\theta)} \tag{4}$$

For this equation, the value of $(\alpha + \theta)$ should be less than δ_0, or the D_{t2} is negative, which has no significance.

To compare D_{t1} and D_{t2}, let

$$\lambda_1 = D_{t2}/D_{t1} = \frac{\sin\delta_0 \sin(\delta_0-\theta)}{\sin(\delta_0-\alpha)\sin(\delta_0-\theta-\alpha)} \tag{5}$$

Because the value of $(\alpha + \theta)$ is less than the value of δ_0, $\sin(\delta_0)$ is larger than $\sin(\delta_0 - \alpha)$ and $\sin(\delta_0 - \theta)$ is larger than $\sin(\delta_0 - \alpha - \theta)$, which indicate that the value of λ_1 is larger than 1. That is to say, for the same values of δ_0 and θ, the synthetic basal detachment produce greater total displacement than the horizontal basal detachment ($D_{t2} > D_{t1}$).

In the case of antithetic basal detachment, by using the law of sines for triangle ABC in Figure 2(e), we obtain

$$L_t = \mathrm{AB} = L_0 \frac{\sin(180-\delta_0)}{\sin(180-\delta_0-\alpha)} = \frac{L_0 \sin\delta_0}{\sin(\delta_0+\alpha)} \tag{6}$$

After rotation, by applying the law of sines to triangle AA B in Figure 2(f), the total displacement (BB') is determined by

$$D_{t3} = \mathrm{BB}' = L_t \frac{\sin\theta}{\sin(\delta_3+\alpha)} = \frac{L_t \sin\theta}{\sin(\delta_0-\theta+\alpha)} = \frac{L_0 \sin\delta_0 \sin\theta}{\sin(\delta_0+\alpha)\sin(\delta_0+\alpha-\theta)} \tag{7}$$

For this equation, the value of θ should be less than $\delta_0 + \alpha$, or the D_{t2} is negative, which has no significance for normal faults.

To compare D_{t1} and D_{t3}, let

$$\lambda_2 = D_{t3}/D_{t1} = \frac{\sin\delta_0 \sin(\delta_0 - \theta)}{\sin(\delta_0 + \alpha)\sin(\delta_0 - \theta + \alpha)} \tag{8}$$

If the angle of the basal detachment α is less than 20˚ and δ_0 is equal to about 60˚, then $(\delta_0 + \alpha)$ is less than 90˚. In this way sin (δ_0) is less than $\sin(\delta_0 + \alpha)$ and $\sin(\delta_0 - \theta)$ is less than $\sin(\delta_0 + \alpha - \theta)$. This indicates that the value of λ_2 is less than 1. In other words, for the same values of δ_0 and θ, the antithetic basal detachment produces smaller total displacement than the horizontal basal detachment ($D_{t3} < D_{t1}$).

2.2. Vertical Shear Model

The second model of rotation is the vertical shear mechanism proposed by Westaway and Kusznir (1993) [22], who argued that the internal deformation within a block bounded by faults is due to vertical shear (**Figure 3(a)** and **Figure 3(b)**). According to the vertical shear model of Westaway and Kusznir (1993) [22], if the bed tilt (θ), and present dip of the fault (δ_4) are known, the original fault dip (δ_0) are calculated by

$$\tan\delta_0 = \tan\theta + \tan\delta_4 \tag{9}$$

Therefore, the fault rotation is

$$\gamma_{t2} = \delta_0 - \delta_4 = \arctan(\tan\theta + \tan\delta_4) - \delta_4 \tag{10}$$

The vertical simple shear causes the initially horizontal surface between faults to be progressively tilted by an angle θ. Thus, the final length (L_b) of a bed is AB′. Using trigonometry,

$$L_b = \mathrm{AB}' = L_0/\cos\theta \tag{11}$$

Then, according to the law of sines the total displacement (D_{t4}) is

$$D_{t4} = \mathrm{AD}' = L_0 \frac{\sin\theta}{\sin\delta_4 \cos\theta} \tag{12}$$

Combining Equations (2) and (12), we define

$$\lambda_3 = D_{t4}/D_{t1} = \frac{\sin\delta_1}{\sin\delta_4 \cos\theta} = \frac{\sin(\delta_0 - \theta)}{\sin\left[\arctan(\tan\delta_0 - \tan\theta)\right]\cos\theta} \tag{13}$$

This Equation (13) indicates that the value of D_{t4}/D_{t1} is dependent on the original fault dip δ_0 and bedding angle θ. For given value of δ_0, the value of λ_3 is negatively related to the value of θ (**Figure 3(c)**). For a given value of θ, the curve of λ_3 shows an up convex (**Figure 3(d)**). In all cases, the value of λ_3 is less than 1, which indicates the value of D_{t4} is smaller than D_{t1} ($D_{t4} < D_{t1}$).

2.3. Inclined Shear Model

The third model of rotation is the inclined shear model [23] [24], which propos-

es that the internal deformation within blocks is due to arbitrary oblique shear. To compare this model with the other two models, we first determine the relationship between the final dip and original dip of the fault. The geometrical configuration is shown in Figure 4. The original normal fault is expressed by the equation:

$$z = ax + b \tag{14}$$

For this equation $\tan(\delta_0) = -a$.

The relationship between fault and bed tilting by ideal inclined shear in the limit of infinitesimal distance from the fault is shown in Figure 4(c). In this condition, the fault is assumed to remain planar, with local dip δ_5. After extension (Figure 4(b)) the initially horizontal marker has equation:

$$y = cx + d_2 \tag{15}$$

where $c = \tan\theta$. An adjacent point D on the fault is now located in point A. Now the vertical coordinate u along DB is

$$u = z + \mathrm{DB} \tag{16}$$

For right triangle ACD, AC = y, and $\angle$CAD = β, which is the angle of inclined shear direction, then AD = $y/\cos\beta$. By applying the law of sines to triangle ADB, we obtain that

$$\mathrm{DB} = \frac{\mathrm{AD}\sin(90-\theta-\beta)}{\sin(90+\theta)} = \frac{y\cos(\theta+\beta)}{\cos\theta\cos\beta} = y(1-\tan\theta\tan\beta) \tag{17}$$

Substituting DB into Equation (17) gives

$$\begin{aligned} u &= z + \mathrm{DB} = ax + b + (cx + d_2)(1-\tan\theta\tan\beta) \\ &= (a + c(1-\tan\theta\tan\beta))x + b + d_2(1-\tan\theta\tan\beta) \end{aligned} \tag{18}$$

After the inclined shear, the fault dip δ_5 will satisfy that $\tan(\delta_5) = -(a + c(1 - \tan\theta\tan\beta))$. Substituting for a and c gives:

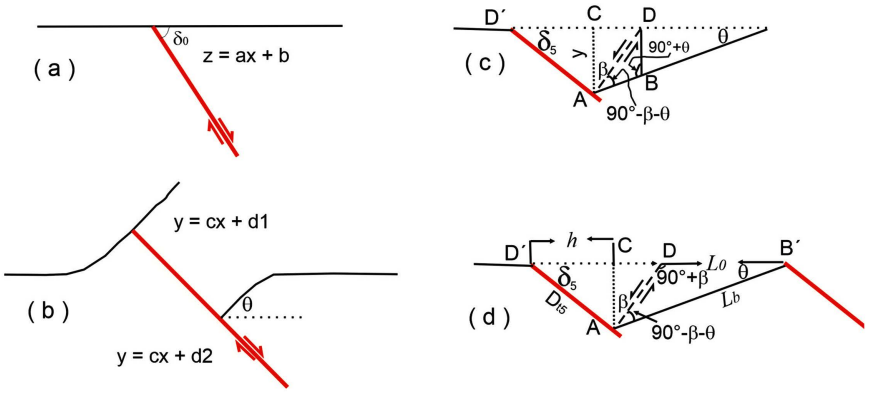

Figure 4. Sketch showing inclined shear. (a) In the initial state, the fault line is assumed to be in the form: $z = ax + b$. (b) After faulting, the bedding near the fault plane has equation $y = cx + d_1$ and $y = cx + d_2$, respectively. (c) A point D near the fault plane moved to point A after faulting. The angle of β is measured from the vertical line to the shear direction. (d) Geometrical configuration for the inclined shear. The heave is different from that for the vertical shear in Figure 3(b).

$$\tan\delta_5 = \tan\delta_0 - \tan\theta\left(1 - \tan\theta\tan\beta\right), \tag{19}$$

Thus,

$$\tan\delta_0 = \tan\delta_5 + \tan\theta\left(1 - \tan\theta\tan\beta\right) \tag{20}$$

For $\beta = 0$, this equation is the same as Equation (9), which indicates that the vertical shear is the case of end member of the inclined shear. Compare this Equation (20) with Equation (9) that assumes vertical shear, we can see that for the same present fault dip ($\delta_5 = \delta_4$) and bedding tilt θ, the calculated original fault dip for inclined shear is smaller than that for the vertical shear. The difference of initial fault dips between the two shear models ($\Delta\delta$) is

$$\Delta\delta = \arctan\left(\tan^2\theta\tan\beta\right) \tag{21}$$

This equation indicates that the value of $\Delta\delta$ is positively related to the bedding tilt θ and the angle of inclined shear (β). The effects of the bedding tilt θ and the angle of inclined shear β are shown in **Figure 5**.

The value of β is negative if measured from vertical line to shear direction (**Figure 4(c)**). As shown in **Figure 4(d)**, DB′ is the initial length of bedding (L_0). Based on the law of sinces for triangle ADB′, the present length (L_b = AB′) of the bedding is:

$$L_b = \mathrm{AB}' = \frac{L_0\sin\left(90+\beta\right)}{\sin\left(90-\beta-\theta\right)} = \frac{L_0\cos\beta}{\cos\left(\beta+\theta\right)} \tag{22}$$

By applying the law of sines to triangle AD B′, the total displacement AD′ can be deduced as

$$\begin{aligned} D_{t5} = \mathrm{AD}' &= L_0\frac{\sin\theta\cos\beta}{\sin\delta_5\cos\left(\beta+\theta\right)} \\ &= \frac{L_0\sin\theta\cos\beta}{\sin\left\{\arctan\left[\tan\delta_0 - \tan\theta\left(1-\tan\theta\tan\beta\right)\right]\right\}\cos\left(\beta+\theta\right)} \end{aligned} \tag{23}$$

To compare D_{t5} with D_{t1}, let $\lambda_4 = D_{t5}/D_{t1}$. Combining Equations (2) and (23), we obtain

$$\lambda_4 = D_{t5}/D_{t1} = \frac{\cos\beta\sin\left(\delta_0-\theta\right)}{\sin\left[\arctan\left(\tan\delta_0 - \tan\theta\left(1-\tan\theta\tan\beta\right)\right)\right]\cos\left(\beta+\theta\right)} \tag{24}$$

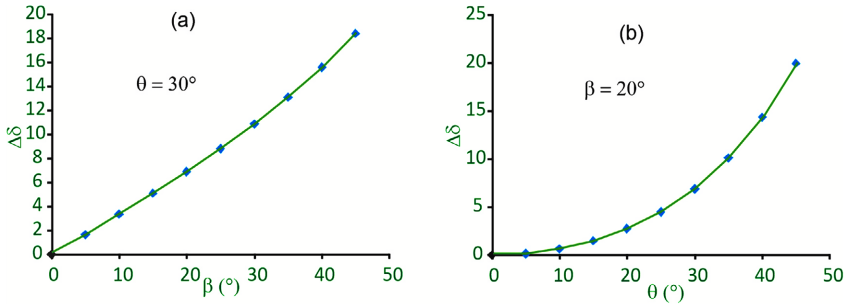

Figure 5. The curve of $\Delta\delta = \arctan\left(\tan^2\theta\tan\beta\right)$ for given $\theta = 30^\circ$ in (a) and $\beta = 20^\circ$ in (b), respectively.

Equation (24) shows that the value of D_{t5}/D_{t1} is dependent on the original fault dip δ_0 and bedding angle θ, and the angle of shear direction β. Generally, the value of λ_4 can be either less than or larger than 1 (Figure 6), which indicates $D_{t5} < D_{t1}$ or $D_{t5} > D_{t1}$. For given values of δ_0 and θ, the value of λ_4 is positively related to the value of β (Figure 6(a)). For given values of δ_0 and β, there are negative relationship between the value of λ_4 and the value of θ (Figure 6(b)). Finally, for given values of θ and β, the value of λ_4 is also negatively related to the value of δ_0 (Figure 6(c)).

Let $\lambda_5 = D_{t5}/D_{t4}$ to compare the value of D_{t5} with D_{t4}. Based on Equations (12) and (23), we have

$$\lambda_5 = D_{t5}/D_{t4} = \frac{\cos\beta\cos\theta\sin\left[\arctan\left(\tan\delta_0 - \tan\theta\right)\right]}{\sin\left[\arctan\left(\tan\delta_0 - \tan\theta\left(1-\tan\theta\tan\beta\right)\right)\right]\cos\left(\beta+\theta\right)} \quad (25)$$

There are three variables in this equation: the original fault dip δ_0, the bedding angle θ, and the angle of shear direction β. For any combination of these three variables, the value of λ_5 is always smaller than 1 (Figure 7). This indicates that for same condition, the inclined shear produces less displacement than the vertical shear. The original fault dip δ_0 does not strongly affect the value of λ_5 (Figure 7(a)). When the value of δ_0 varies from 70˚ to 30˚, the difference of λ_5 is only equal to 0.04 changing from 0.72 to 0.78. On the other hand, the value of λ_5 is negatively related to the value of θ, and is positively related to the value of β (Figure 7(b) and Figure 7(c)).

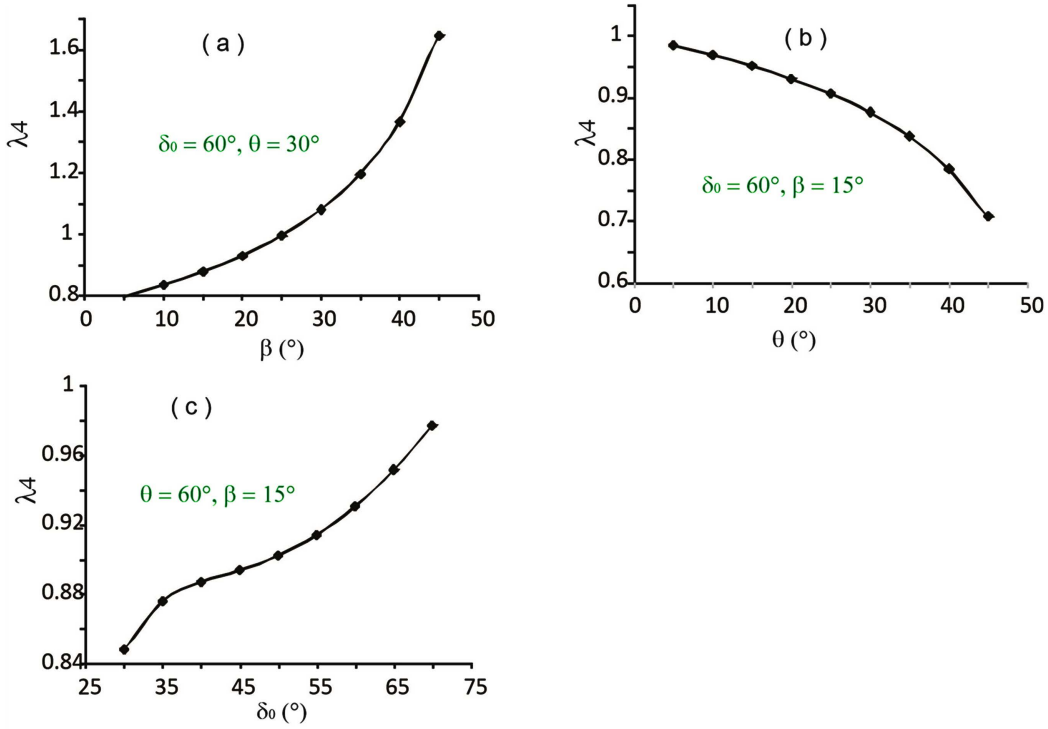

Figure 6. The change of $\lambda_4 = D_{t5}/D_{t1}$ for given conditions. The value of λ_4 can be either larger than or smaller than 1.

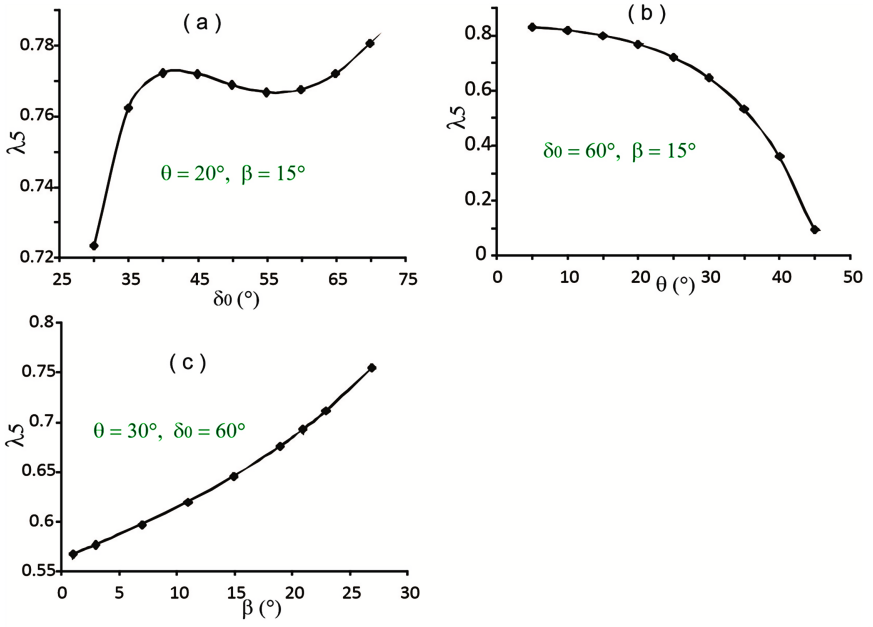

Figure 7. The value of $\lambda_5 = D_{t5}/D_{t4}$ varies with δ_0 in (a), θ in (b), and β in (c), respectively.

3. Horizontal Extension in the Case of Reverse Drag

For any model of block rotation, the horizontal extension is defined as

$$\varepsilon = \left(L_f - L_0\right)/L_0 \tag{26}$$

where L_f is the final horizontal length of the fault block after faulting, and L_0 is the initial horizontal length. For the rigid body mechanism on the horizontal base (**Figure 2(a)** and **Figure 2(b)**), the fault heave is $h_1 = D_{t1}\cos\delta_1 = D_{t1}\cos(\delta_0 - \theta)$. Substituting for D_{t1} from Equation (2), we have $h_1 = L_0\text{ctan}(\delta_0 - \theta)\sin\theta$. Then, the final length is $L_{f1} = h_1 + \text{DB}' = L_0[\cot(\delta_1)\sin(\theta) + \cos(\theta)]$. In this way, the extension is expressed as

$$\varepsilon_1 = \left(L_{f1} - L_0\right)/L_0 = \text{ctan}\left(\delta_0 - \theta\right)\sin\theta + \cos\theta - 1 \tag{27}$$

For the vertical shear, the horizontal distance between the footwall cutoff of one fault and the hanging-wall cutoff in the next fault will remain constant over time, having its initial value (L_0 in **Figure 3(b)**). In this way, we have $\text{DB}' = L_0$ and the heave is $h_2 = \text{D}'\text{D} = D_{t4}\cos\delta_4$. The value of D_{t4} is substituted into this equation, we have $h_2 = L_0\text{ctan}\delta_4\tan\theta$, then $L_{f4} = \text{DB}' + \text{D}'\text{D} = L_0(\text{ctan}\delta_4\tan\theta + 1) = L_0(\text{ctan}(\arctan(\tan\delta_0 - \tan\theta))\tan\theta + 1) = L_0(\tan\theta/(\tan\delta_0 - \tan\theta) + 1)$. Therefore, the horizontal extension is

$$\varepsilon_4 = \left(L_{f4} - L_0\right)/L_0 = \tan\theta/\left(\tan\delta_0 - \tan\theta\right) \tag{28}$$

To compare the value of ε_4 with ε_1, let $\rho_1 = \varepsilon_4/\varepsilon_1$. From Equations (27) and (28), we deduce

$$\rho_1 = \varepsilon_4/\varepsilon_1 = \frac{\tan\theta}{\left(\tan\delta_0 - \tan\theta\right)\left(\text{ctan}\left(\delta_0 - \theta\right)\sin\theta + \cos\theta - 1\right)} \tag{29}$$

This equation indicates that the value of $\varepsilon_2/\varepsilon_1$ is dependent on the original

fault dip δ_0 and bedding angle θ. For given values of δ_0, the value of ρ_1 is negatively related to the value of θ (Figure 8(a)). For given value of θ, the value of ρ_1 is also negatively related to the value of δ_0 (Figure 8(b)). For all combinations of fault dip δ_0 and bedding angle θ, the value of ρ_1 is less than 1, which indicates the value of ε_4 is smaller than ε_1 ($\varepsilon_4 < \varepsilon_1$). Note that for the same values of fault dip δ_0 and bedding angle θ, the value of ρ_1 is not equal to λ_3, that is, $\varepsilon_4/\varepsilon_1 \neq D_{t4}/D_{t1}$. For example, given $\delta_0 = 60^\circ$ and $\theta = 20^\circ$, $\rho_3 = 0.766$, whereas $\lambda_3 = 0.847$.

Now we consider the inclined shear in Figure 4(d), the value of final length L_{f5} = D Ď + DB′ = D Č + CD + L_0. Because D Č = $D_{t5}\cos\delta_5$ and CD = $A\text{C}\tan\beta$ = D Č$\tan\delta_5\tan\beta$, $L_{f5} = D_{t5}\cos\delta_5(1 + \tan\delta_5\tan\beta) + L_0$. Substituting for D_{t5} gives

$$L_{f5} = L_0\left(\frac{\sin\theta\cos\beta\left(1+\tan\delta_5\tan\beta\right)}{\tan\delta_5\cos\left(\beta+\theta\right)}+1\right) \tag{30}$$

Thus, the extension is

$$\varepsilon_5 = \frac{L_{f5}-L_0}{L_0} = \frac{\sin\theta\cos\beta\left(1+\tan\delta_5\tan\beta\right)}{\tan\delta_5\cos\left(\beta+\theta\right)} \tag{31}$$

Apply the equation $\cos(\beta + \theta) = \cos\beta\cos\theta - \sin\beta\sin\theta$ to Equation (31) and rearrange it, we obtain

$$\varepsilon_5 = \frac{\tan\theta\left(1+\tan\delta_5\tan\beta\right)}{\tan\delta_5\left(1-\tan\theta\tan\beta\right)} \tag{32}$$

where $\tan\delta_5$ is calculated by Equation (19), which depends on the values of δ_0 and β. We define $\rho_2 = \varepsilon_5/\varepsilon_1$, the expression of ρ_2 is

$$\rho_2 = \frac{\tan\theta(1+\tan\delta_5\tan\beta)}{\tan\delta_5\left(1-\tan\theta\tan\beta\right)\left(c\tan\left(\delta_0-\theta\right)\sin\theta+\cos\theta+1\right)} \tag{33}$$

For all combinations of fault dip δ_0, the angle of inclined shear β, and bedding angle θ, the value of ρ_2 can be less than or greater than 1 (Figure 9). For given value of θ, the value of ρ_2 is negatively related to the value of δ_0 (Figure 9(a)). On the other hand, the value of ρ_2 is positively related to the value of θ and β (Figure 9(b) and Figure 9(c)). Compare Figure 8 with Figures 10(a)-(c), there are two differences between ρ_2 and λ_4. First, the range of ρ_2 is larger than that of λ_4. The value of λ_4 is less than 2, whereas the value of ρ_2 can be greater than 10. Second, the curves of ρ_2 and λ_4 have opposite tendency related to δ_0, θ and β.

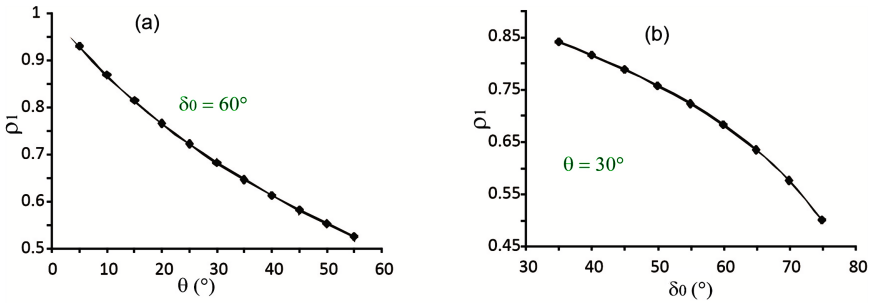

Figure 8. The change of $\rho_1 = \varepsilon_4/\varepsilon_1$ for given $\delta_0 = 60^\circ$ in (a) and $\theta = 30^\circ$ in (b). The value of ρ_1 is always smaller than 1.

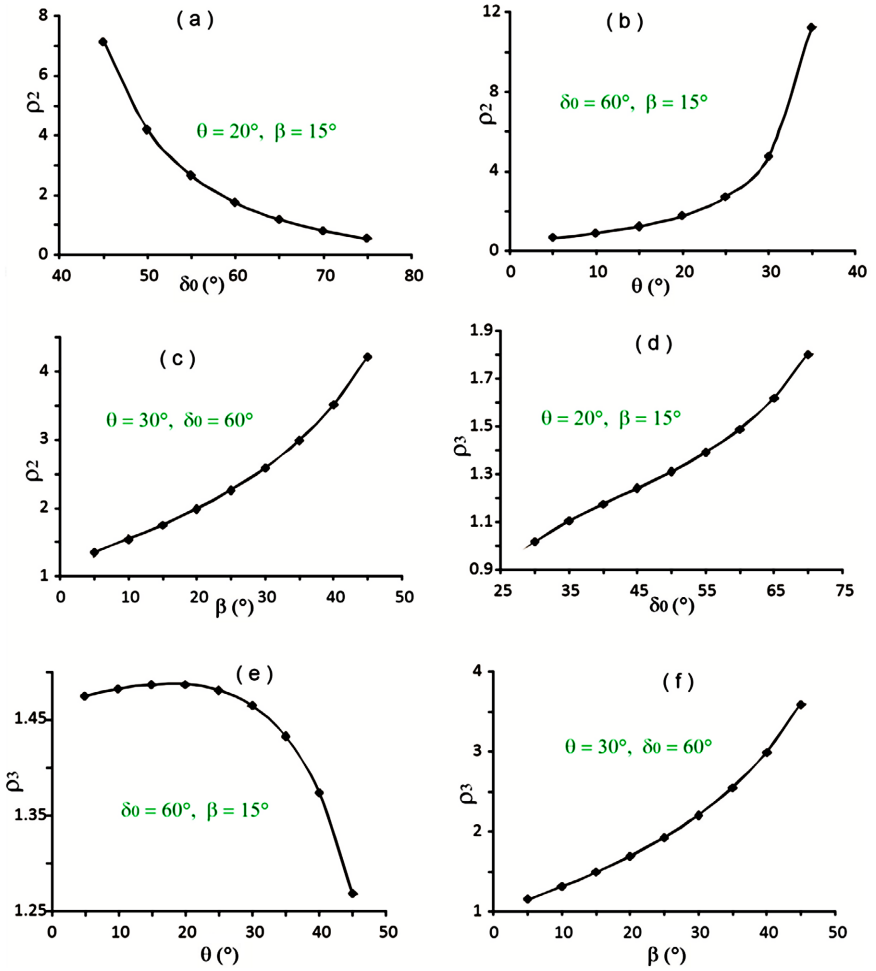

Figure 9. The change of $\rho_2 = \varepsilon_5/\varepsilon_1$ and $\rho_3 = \varepsilon_5/\varepsilon_4$ for given conditions. The value of ρ_2 can be either larger than or smaller than 1 depending on combination of δ_0, θ, α and β. For arbitrary combination of δ_0, θ, α and β, the value of ρ_3 is always larger than 1.

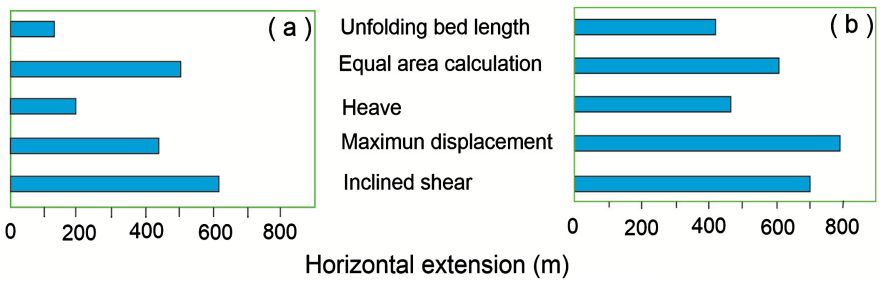

Figure 10. Estimation of the amount of extension using different methods across a listric fault in the Norwegian margin (a) and the Gulf Coast (b) (modified from [25]).

On the other hand, we define $\rho_3 = \varepsilon_5/\varepsilon_4$, the expression of ρ_3 is

$$\rho_3 = \frac{(\tan\delta_0 - \tan\theta)(1 + \tan\delta_5 \tan\beta)}{\tan\delta_5 (1 - \tan\theta \tan\beta)} \tag{34}$$

There are three variables in this equation: the original fault dip δ_0, the bedding angle θ, and the angle of shear direction β. For any combination of these three

variables, the value of ρ_3 is always larger than 1 (**Figures 9(d)-(f)**). This indicates that for same condition, the inclined shear produces larger extension than the vertical shear. On the other hand, the value of ρ_3 is positively related to the value of β and δ_0 (**Figure 9(d)** and **Figure 9(f)**). For given value of β and δ_0, the curve of ρ_3 shows a down convex curve (**Figure 9(e)**). Compare **Figure 7** and **Figures 9(d)-(f)**, one can see the curve of λ_5 and ρ_3 show different tendency. The values of λ_5 and ρ_3 are quite different: $\lambda_5 < 1$, whereas $\rho_3 > 1$. This indicates although the displacement caused by the inclined shear is smaller than that by the vertical shear, the extension from the inclined shear is larger than from the vertical shear.

4. Discussion

The rigid body model indicates that there is no internal deformation within the blocks. The simple shear models represent internal deformation. For listric normal faults, there are some other techniques to estimate horizontal extension. Exception for the simple shear method, Poblet and Bulnes (2005) [25] discussed six geometric mechanisms to estimate horizontal extension in simple listric normal faults. They are: 1) unfolding sinuous bed lengths, e = structural width-folded bed length; 2) equal-area calculation, e = dropped area/detachment depth; 3) heave, e = heave; 4) maximum displacement on the fault, e = displacement on the fault; 5) extensional fault-bend folding, e = distance between hanging-wall active and inactive axial surfaces along the lower flat; and 6) lost-area diagram, e = slop of best-fit line across area versus depth of several horizons to a reference level. By physical experiments, they showed that the estimated extension from different methods yield different magnitudes. Although the maximum displacement method and the extensional fault-bend folding method yield the best estimates of the amount of horizontal extension, all estimated extensions are less than the true values. These results indicate that hidden extensions may occur on faults below the smaller scale during progressive deformation [26].

Estimation of extension of field examples from the Norwegian margin fault and the Gulf Coast fault are shown in **Figure 10**. Different methods yield evident different results. In both examples, the maximum displacement and inclined shear methods have the largest amounts of extension. Here, the values of fault shear used to apply the inclined shear are 40˚ for the Norwegian margin fault, and 20˚ for Gulf Coast fault. These results are different from the results of physical experiments [25].

5. Conclusions

For reverse drags, three mechanisms were considered in our analysis: rigid body rotation, vertical shear, and inclined shear. The results allow us to obtain the following conclusions.

The established equations show that among the three subcases of rigid body model, the total displacement in the case of the synthetic base (D_{t2}) is the largest,

that in the case of the horizontal base (D_{t1}) is moderate, and that in the case of the antithetic base (D_{t3}) is the smallest based on the same original parameters. Also, it is shown that the value of (D_{t1}) is larger than the displacement for the vertical shear (D_{t4}). the displacement for the inclined shear (D_{t5}) can be either larger than or less than the value of (D_{t1}) depending on combination among the original fault dip δ_0, bedding angle θ, and the angle of shear direction β. For all original parameters, the value of D_{t5} is less than the value of D_{t4}. As for horizontal extension due to normal faulting, we find that the inclined shear produces largest value, the rigid body model with horizontal detachment produces the smallest value, and the vertical shear model produces moderate value.

Acknowledgements

This work was supported by the PAPIIT project IN102020 of National University of Mexico, the project 2020B1515020016 (Natural Science Foundation for Youths of Guangdong), and the project 2022YFC3102200 (National Key Research and Development Program of China).

Conflicts of Interest

The authors declare no conflicts of interest regarding the publication of this paper.

References

[1] Anderson, E.M. (1951) The Dynamic of Faulting and Dyke Formation. Oliver and Boyd, Edinburgh, 206 p.

[2] Jaeger, J.C., Cook, N.G.W. and Zimmerman, R.W. (2007) Fundamentals of Rock Mechanics. Blackwell Publishing, Hoboken.

[3] Sibson, R.H. (1985) A Note on Fault Reactivation. *Journal of Structural Geology*, **7**, 751-754. https://doi.org/10.1016/0191-8141(85)90150-6

[4] Hamblin, W.K. (1965) Origin of "Reverse Drag" on the Downthrown Side of Normal Faults. *Bulletin of the Geological Society of America*, **76**, 1145-1164. https://doi.org/10.1130/0016-7606(1965)76[1145:OORDOT]2.0.CO;2

[5] Schlische, R.W. (1995) Geometry and Origin of Fault-Related Folds in Extensional Settings. *AAPG Bulletin*, **79**, 1661-1678. https://doi.org/10.1306/7834DE4A-1721-11D7-8645000102C1865D

[6] Johnson, A.M. (1970) Physical Processes in Geology. Freeman, Cooper and Co., San Francisco, 577 p.

[7] Mitra, S. (1993) Geometry and Kinematic Evolution of Inversion Structures. *AAPG Bulletin*, **77**, 1159-1191. https://doi.org/10.1306/BDFF8E2A-1718-11D7-8645000102C1865D

[8] Patton, T.L. (2004) Numerical Models of Growth-Sediment Development above an Active Monocline. *Basin Research*, **16**, 25-39. https://doi.org/10.1111/j.1365-2117.2003.00220.x

[9] Rykkelid, E. and Fossen, H. (2002) Layer Rotation around Vertical Fault Overlap Zones: Observations from Seismic Data, Field Examples, and Physical Experiments. *Marine and Petroleum Geology*, **19**, 181-192.

https://doi.org/10.1016/S0264-8172(02)00007-7

[10] Davis, G.H. (1984) Structural Geology of Rocks and Regions. John Wiley and Sons, New York, 592 p.

[11] Reches, Z. and Eidelman, A. (1995) Drag along Faults. *Tectonophysics*, **247**, 145-156. https://doi.org/10.1016/0040-1951(94)00170-E

[12] Grasemann, B., Martel, S. and Passchier, C. (2005) Reverse and Normal Drag along a Fault. *Journal of Structural Geology*, **27**, 999-1010. https://doi.org/10.1016/j.jsg.2005.04.006

[13] Brandes, C. and Tanner, D.C. (2014) Fault-Related Folding: A Review of Kinematic Models and Their Application. *Earth-Science Reviews*, **138**, 352-370. https://doi.org/10.1016/j.earscirev.2014.06.008

[14] Homberg, C., Schnyder, J., Roche, V., Leonardi, V. and Benzaggagh, M. (2017) The Brittle and Ductile Components of Displacement along Fault Zones. *Geological Society, London, Special Publications*, **439**, 395-412. https://doi.org/10.1144/SP439.21

[15] Delogkos, E., Saqab, M.M., Walsh, J.J., Roche, V. and Childs, C. (2020) Throw Variations and Strain Partitioning Associated with Fault-Bend Folding along Normal Faults. *Solid Earth*, **11**, 935-945. https://doi.org/10.5194/se-11-935-2020

[16] Withjack, M.O., Islam, Q.T. and La Pointe, P.R. (1995) Normal Faults and Their Hanging-Wall Deformation: An Experimental Study. *AAPG Bulletin*, **79**, 1-17. https://doi.org/10.1306/8D2B1494-171E-11D7-8645000102C1865D

[17] Ferrill, D.A., Morris, A.P., Sims, D.W., Waiting, D.J. and Hasegawa, S. (2005) Development of Synthetic Layer Dip Adjacent to Normal Faults. In: Sorkhabi, R. and Tsuji, Y., Eds., *Faults, Fluid Flow, and Petroleum Traps*, American Association of Petroleum Geologists, Tulsa, Memoirs, No. 85, 125-138.

[18] Tearpock, D.J. and Bischke, R.E. (2003) Applied Subsurface Geological Mapping. Prentice Hall, Hoboken.

[19] Hesthammer, J. and Fossen, H. (2000) Uncertainties Associated with Fault Sealing Analysis. *Petroleum Geoscience*, **6**, 37-45. https://doi.org/10.1144/petgeo.6.1.37

[20] Chen, Y.G., Lai, K.Y., Lee, Y.H., Suppe, J., Chen, W.S., Lin, Y.N.N., Wang, Y., Hung, J.H. and Kuo, Y.T. (2007) Coseismic Fold 315 Scarps and Their Kinematic Behavior in the 1999 Chi-Chi Earthquake Taiwan Region. *Journal of Geophysical Research: Solid Earth*, **112**, B03S02. https://doi.org/10.1029/2006JB004388

[21] Axen, G.J. (1988) The Geometry of Planar Domino-Style Normal Faults above a Dipping Basal Detachment. *Journal of Structural Geology*, **10**, 405-411. https://doi.org/10.1016/0191-8141(88)90018-1

[22] Westaway, R. and Kusznir, N. (1993) Fault and Bed "Rotation" during Continental Extension: Block Rotation or Vertical Shear? *Journal of Structural Geology*, **16**, 753-770. https://doi.org/10.1016/0191-8141(93)90060-N

[23] Xu, S.S., Nieto-Samaniego, A.F. and Alaniz-Álvarez, S.A. (2004) Tilting Mechanism in Domino Faults of the Sierra de San Miguelito, Central Mexico. *Geologica Acta*, **3**, 189-201.

[24] White, N.J., Jackson, J.A. and Mckenzie, D.P. (1986) The Relationship between the Geometry of Normal Faults and That of the Sedimentary Layers in Their Hanging Walls. *Journal of Structural Geology*, **8**, 879-909. https://doi.org/10.1016/0191-8141(86)90035-0

[25] Poblet, J. and Bulnes, M. (2005) Fault-Slip, Bed-Length and Area Variations in Experimental Rollover Anticlines over Listric Normal Faults: Influence in Extension and Depth to Detachment Estimations. *Tectonophysics*, **396**, 97-117.

https://doi.org/10.1016/j.tecto.2004.11.005

[26] Kautz, S.A. and Sclater, J.G. (1988) Internal Deformation in Clay Models of Extension by Block Faulting. *Tectonics*, **7**, 823-832. https://doi.org/10.1029/TC007i004p00823